



Universiteit
Leiden
The Netherlands

Insulin resistance in obese patients with type 2 diabetes mellitus : effects of a very low calorie diet

Jazet, I.M.

Citation

Jazet, I. M. (2006, April 11). *Insulin resistance in obese patients with type 2 diabetes mellitus : effects of a very low calorie diet*. Retrieved from <https://hdl.handle.net/1887/4366>

Version: Corrected Publisher's Version

License: [Licence agreement concerning inclusion of doctoral thesis in the Institutional Repository of the University of Leiden](#)

Downloaded from: <https://hdl.handle.net/1887/4366>

Note: To cite this publication please use the final published version (if applicable).

CHAPTER 8

Effect of loss of 50% overweight on insulin-stimulated glucose disposal, insulin signalling and intramyocellular triglycerides in obese, insulin-treated type 2 diabetic patients using a very low calorie diet.

Ingrid M. Jazet¹, Gert Schaart², D. Margriet Ouwens³, Hanno Pijl¹, J. Antonie Maassen³, A. Edo Meinders¹

Departments of ¹General Internal Medicine and ²Molecular Cell Biology, Leiden University Medical Centre, Leiden, The Netherlands. ³Department of Movement Sciences, Maastricht University, Maastricht, The Netherlands.

In preparation for submission together with Chapter 7

ABSTRACT

To investigate the effect of considerable weight loss on skeletal muscle glucose disposal, both at the whole body and at the molecular level, 10 obese (BMI 40.2 ± 1.6 kg/m² [mean \pm SEM]) insulin-treated type 2 diabetic patients (HbA_{1c} $7.7 \pm 0.4\%$, FPG 11.1 ± 0.8 mmol/L) were studied during a very low calorie diet (VLCD, 450 kCal/day) on day 2 and again after losing 50% of their overweight (50% OWR). Oral blood glucose-lowering agents and insulin were discontinued 3 weeks prior to the VLCD and at the start of the VLCD, respectively. Endogenous glucose production (EGP) and whole-body glucose disposal ($6,6\text{-}^2\text{H}_2\text{-glucose}$), lipolysis ($^2\text{H}_5\text{-glycerol}$) and substrate oxidation rates were measured on both study days in basal and hyperinsulinaemic (insulin infusion rate 40mU/m² per minute) euglycaemic conditions. In addition, skeletal muscle biopsies were obtained from the vastus lateralis muscle, in the basal situation and 30 min after the start of the insulin infusion for determination of insulin signalling, insulin-mediated expression of GLUT-4 and FAT/CD36 at the cell membrane and intramyocellular triglyceride content.

Weight reduction (20.3 ± 2.2 kg from day 2 to day 50% OWR) not only normalised basal EGP, but also improved insulin sensitivity, especially insulin-stimulated glucose disposal (18.8 ± 2.0 to 39.1 ± 2.8 $\mu\text{mol.kgFFM}^{-1}.\text{min}^{-1}$, $p = 0.001$). At the myocellular level, insulin-stimulated phosphatidylinositol 3'-kinase (PI3K)-activity over basal was significantly higher after weight loss. In addition, 2 down-stream effectors, AS160 and PRAS40, showed an absolute increase after weight loss. The improvement in insulin signalling was accompanied by a tendency for increased GLUT-4 content at the sarcolemma during hyperinsulinaemia. Intramyocellular triglyceride content decreased, with no significant change in insulin-stimulated sarcolemmal FAT/CD36 content. Time to weight loss of 50% overweight was negatively correlated with the number of type I muscle fibres at baseline.

In conclusion, the increase in insulin-stimulated glucose disposal after considerable weight loss in obese type 2 diabetic patients is associated with a tendency to improved insulin signalling at the level of PI3K, and a significant improvement in signalling towards the more downstream components, AS160 and PRAS40. The observed decrease in intramyocellular triglyceride content might have contributed to this effect. The fact that GLUT-4 content at the sarcolemma did not change significantly indicates that it is not GLUT-4 content that is important in insulin-stimulated glucose disposal, but rather its insulin-stimulated translocation or the intrinsic activity of GLUT-4. Alternatively, another glucose transporter or increased glucose uptake in adipose tissue might be responsible for the observed increase in insulin-stimulated glucose uptake.

INTRODUCTION

About 80% of insulin-stimulated glucose disposal takes place in skeletal muscle¹, with glucose transport over the membrane as the rate limiting step². In type 2 diabetic patients, insulin-stimulated glucose disposal is disturbed due to defects in the insulin-signalling pathway regulating the translocation of the glucose transporter GLUT-4 to the cell membrane. Notably, defects in insulin-induced phosphorylation of insulin receptor substrate-1 (IRS-1) and phosphatidylinositol 3-kinase (PI3K)³⁻⁶ and in translocation of GLUT-4 to the cell membrane^{7,8} have been found in skeletal muscle of patients with type 2 diabetes, whereas total GLUT-4 protein and mRNA levels in type 2 diabetic patients have repeatedly shown to be normal^{9,10}. The involvement of the PI3K substrate protein kinase B (PKB/Akt) in skeletal muscle insulin resistance is less clear, as is illustrated by studies reporting either normal^{4,11} or impaired activation^{12,13} by insulin. However, the recently characterised Akt substrate 160 (AS160)^{14,15} has been implicated in linking PKB/Akt activation to GLUT-4¹⁶ trafficking and insulin-mediated AS160 phosphorylation is impaired in skeletal muscle of type 2 diabetic patients¹⁷. Collectively these studies highlight the importance of the PI3K-PKB/AKT-AS160-signalling pathway regulating GLUT-4 trafficking.

Caloric restriction and weight loss both improve hyperglycaemia in type 2 diabetic patients. We previously reported that a 2-day very low calorie diet (VLCD, Modifast[®], 450 kCal/day) decreased basal endogenous glucose production (EGP) in obese insulin-treated type 2 diabetic patients in whom all blood glucose-lowering medication was discontinued¹⁷. These changes were neither accompanied by an improvement in whole-body peripheral insulin sensitivity, nor by changes in insulin signalling, fuel transporter (GLUT-4, FAT/CD 36) localisation and triglyceride content in skeletal muscle biopsies¹⁹.

In the present study, we assessed whether a prolonged VLCD in obese insulin-treated type 2 diabetic patients leading to substantial weight loss (50% of overweight) has a different blood glucose-lowering mechanism as compared to caloric restriction only (2-day VLCD). During the study all blood glucose-lowering agents, including insulin, were discontinued. Insulin sensitivity was determined by hyperinsulinaemic euglycaemic clamp (insulin infusion: 10 minute prime followed by a constant rate of 40 mU/m²/min) on day 2 of the VLCD and after loss of 50% of the overweight. Insulin signalling, insulin-mediated expression of GLUT-4 and FAT/CD36 at the cell membrane and intramyocellular triglyceride content were determined in skeletal muscle biopsies obtained on both study days in the basal situation and 30 minutes after the start of the insulin infusion.

RESEARCH DESIGN AND METHODS

Subjects

10 obese (BMI 40.2 ± 1.6 kg/m², [mean \pm SEM]) patients with type 2 diabetes mellitus (FPG 11.1 ± 0.8 mmol/L, HbA_{1c} $7.7 \pm 0.4\%$, duration of type 2 diabetes mellitus 8 ± 3 years), 8 women and 2 men (age 54 ± 3 years) participated in this study, which was approved by the Medical Ethical Committee of Leiden University Medical Centre. Written informed consent was obtained from all patients after the study was explained.

Patients had to use at least 30 units of insulin per day (mean 94 ± 14 units/day, 8 patients also used metformin and 2 patients used rosiglitazone with the insulin therapy) and had to have a BMI > 30 kg/m². In addition, patients had to have remaining endogenous insulin secretion defined as a fasting plasma C-peptide level of more than 0.8 ng/mL or a 2-fold increase of the basal C-peptide level after administration of 1 mg glucagon i.v.

Patients had to have a stable body weight for at least 3 months and were instructed not to alter life style habits (eating, drinking, exercise) from screening until the start of the study. None of the patients were smokers and the use of other medication (than that used specific for the treatment of hyperglycaemia) known to alter glucose or lipid metabolism was prohibited.

Diet and protocol outline

Three weeks before the start of the study, all oral blood glucose-lowering medication was discontinued. At day -1 only short acting insulin was given, evening doses of intermediate- and long-acting insulin were omitted. On day 0, patients started a VLCD (450 kCal/day) consisting of 3 sachets of Modifast® (Nutrition & Santé, Antwerpen, Belgium) per day, providing about 50 gram protein, 50 to 60 g carbohydrates, 7 to 9 g lipids, and 10 g of dietary fibres. Insulin therapy remained stopped from the start of the VLCD on. After 48 hours of the VLCD patients were admitted to the research centre for the metabolic studies (day 2) as outlined below. After this study day patients continued the VLCD until they had lost 50% of their overweight (see *Calculations*). Then the second study day took place (day 50% overweight-reduced [OWR]).

During the VLCD patients visited the research centre on a weekly basis for measurement of body weight, waist-hip ratio, blood pressure and blood glucose regulation.

Study days

All studies started at 7:00 AM after an overnight fast. Length (meters [m]), weight (kilograms [kg]) and body mass index (BMI = weight (kg) / length² (m)) were measured according to WHO recommendations²⁰. Body fat mass (FM) and fat free mass (FFM) were measured by Bioelectrical Impedance Analysis (BIA, Bodystat® 1500, Bodystat Ltd., Douglas, Isle of Man, UK). The impedance measurements were performed first thing in the morning after subjects had voided and while they were fasting and resting in bed.

Metabolic studies were performed as described previously¹⁸. In short, basal rates of glucose and glycerol turnover were assessed after 3 hours of an adjusted primed ($17.6 \mu\text{mol/kg} \times \text{actual plasma glucose concentration (mmol/L)}/5(\text{normal plasma glucose})$)²¹ continuous ($0.33 \mu\text{mol/kg per min}$) infusion of $[6,6\text{-}^2\text{H}_2]$ -glucose (Cambridge Isotopes, enrichment 99.9% Cambridge, USA) and 1.5 hours of a primed ($1.6 \mu\text{mol/kg}$) continuous ($0.11 \mu\text{mol/kg per min}$) infusion of $[^2\text{H}_5]$ -glycerol (Cambridge Isotopes, Cambridge, USA). Insulin-stimulated rates of glucose and glycerol turnover were assessed after 4.5 hours of a hyperinsulinaemic euglycaemic clamp (Actrapid®, Novo Nordisk Pharma, Alphen aan de Rijn, The Netherlands, rate $40 \text{ mU/m}^2/\text{min}$ ²²). Glucose values were clamped at 5 mmol/L via the infusion of a variable rate of 20% glucose enriched with 3% $[6,6\text{-}^2\text{H}_2]$ -glucose.

Blood chemistry

Serum insulin was measured with an immunoradiometric assay (IRMA, Biosource, Nivelles, Belgium). The detection limit was 3 mU/L and the interassay coefficient of variation was below 6%.

Serum C-peptide was measured with a radioimmuno assay from Linco Research, St. Charles MO, USA. The interassay coefficient of variation (CV) varied between 4.2 and 6.0% at different levels with a sensitivity of 0.03 nmol/L . Serum triglycerides were determined with a fully automated Hitachi 747 system (Hitachi, Tokyo, Japan).

Serum glucose and $[6,6\text{-}^2\text{H}_2]$ -glucose as well as serum glycerol and $[^2\text{H}_5]$ -glycerol were determined in a single analytical run, using gas chromatography coupled to mass spectrometry as described previously^{23,24}.

Serum non-esterified fatty acids (NEFAs) were measured using the enzymatic colorimetric acyl CoA synthase/acyl-CoA oxidase assay (Wako Chemicals, Neuss, Germany) with a detection limit of 0.03 mmol/L . The interassay coefficient of variation was below 3%.

Muscle biopsies

Muscle biopsies were taken from the vastus lateralis muscle after localised anaesthesia with 1% lidocaine, with a modified Bergström needle (Maastricht Instruments, Maastricht, The Netherlands) using applied suction²⁵. The muscle biopsies were taken in the basal situation (8:00 AM, i.e., 1 hour after patients came in and were in a semirecumbent position) and 30 minutes²⁶ after the start of the insulin infusion (10 minute prime followed by a constant rate of $40 \text{ mU/m}^2/\text{min}$), while blood glucose levels were kept at initial values during these first 30 minutes *via* the infusion of 20% glucose at a variable rate. Muscle samples were snap-frozen in isopentane chilled on dry ice and stored at -80°C until further analysis.

Insulin Signalling

Muscle biopsies were homogenised in PI3K lysis buffer using an ultraturrax mixer and centrifuged (15 minutes; $14,000 \text{ rpm}$; 4°C), then protein content was determined using a BCA-kit

(Pierce, Rockford, IL)²⁷. Insulin receptor substrate-1 (IRS-1) was immunoprecipitated overnight (4°C) from 1.5 mg protein using IRS-1 antibody K6, and PI3K-activity was determined as described previously²⁷.

To determine expression and phosphorylation of other components of the insulin signaling system, proteins (25 µg/lane) were separated by sodium dodecyl sulfate (SDS)-polyacrylamide gel electrophoresis and blotted on polyvinylidene difluoride-membranes (Millipore, Bedford, MA). Filters were incubated overnight (4°C) with IRS-1 K6 and Akt-1 antibody (Upstate, Lake Placid, USA), anti-phospho-Proline rich Akt substrate 40 (PRAS40)-Thr246 (#44-100G), anti-phospho-AS160 (#44-1071G) (Biosource International, Camarillo, CA, USA) and anti-AS160/TBC1D4-antibody (Abcam, Ltd, Cambridge, UK). Bound antibodies were detected using appropriate horseradish peroxidase-conjugated secondary antibodies (Promega, Madison, WI, USA) in a 1:10.000 dilution, followed by visualization by enhanced chemiluminescence. Blots were quantitated by densitometric analysis of the films using Scion Image beta 4.02 software.

Oil Red O staining

According to Koopman *et al.*²⁸ tissue sections of basal biopsies were stained with Oil Red O (ORO) combined with a double-immunofluorescence assay. Briefly, after fixation with 4% formaldehyde in mQ-water, sections were incubated for 45 minutes at room temperature with a mixture of the polyclonal rabbit antiserum directed to laminin (L-9393, Sigma, Sigma-Aldrich Chemie, Zwijndrecht, The Netherlands) and a mouse monoclonal antibody directed against adult human slow myosin heavy chain (Developmental Studies Hybridoma Bank, Iowa City, IO, USA). After three washing steps with phosphate-buffered saline (PBS), sections were incubated for 30 minutes at room temperature with the appropriate secondary antibodies, i.e., Goat anti-Rabbit AlexaFluor350 and Goat anti-Mouse IgM AlexaFluor488 (Molecular Probes, Invitrogen, Breda, The Netherlands). After three final washing steps with PBS, sections were stained with Oil Red Oil according to Koopman *et al.*²⁸. Finally, the sections were mounted in Mowiol.

Images were examined in a Nikon E800 microscope (Uvikon, Bunnik, the Netherlands) and were digitally captured using a 1.3 Megapixel Basler A101C progressive scan colour CCD colour camera, driven by LUCIA laboratory image processing and analysis software (Laboratory Imaging, Prague, Czech Republic).

Oil Red O epifluorescence signal was quantified for each muscle cell of each cross section as described before²⁹. Lipid droplet density was calculated by dividing the total number of droplets by the total (IMCL) area measured.

Sodium dodecyl sulphate-polyacrylamide gel electrophoresis and Western blotting for FAT/CD36 and GLUT-4

For Western blotting analyses, muscle membrane fractions and total muscle protein fractions were prepared as described before for GLUT-4³⁰ and FAT/CD36^{19,31} in biopsies taken during the insulin-stimulated situation.

Equal amounts of proteins were loaded on 10% polyacrylamide SDS-gels and after electrophoretic separation, the proteins were transferred to nitrocellulose in Western blotting. Then the blots were preincubated for 60 min with Odyssey Blocking Buffer (Licor, Westburg, Leusden, The Netherlands) 1:1 diluted in PBS and incubated overnight at room temperature with the polyclonal GLUT-4-BW antibody³⁰ or the MO25 monoclonal antibody specific for FAT/CD36³¹. Then, after incubation with the appropriate secondary antibodies Donkey anti-Rabbit IRDye800 and Donkey anti-Mouse IRDye800 (Rockland, TeBu-bio, Heerhugowaard, The Netherlands), protein bands were detected and quantified with an Odyssey Infrared Imager (Licor). Primary and secondary antibodies were diluted in Odyssey Blocking Buffer. Finally, protein bands were detected and quantified with an Odyssey Infrared.

Calculations

The rate of appearance (R_a) and rate of disappearance (R_d) for glucose and glycerol were calculated using the steady state equation by Steele³² as adapted for stable isotopes using a single compartment kinetic model.

Endogenous glucose production (EGP) during the basal steady state is equal to the R_a of glucose, whereas EGP during the clamp was calculated as the difference between R_a and the glucose infusion rate.

Total lipid and carbohydrate oxidation rates were calculated as described by Simonson and DeFronzo³³. For the conversion of fat oxidation from milligram per kilogram per minute to micromole per kilogram per minute an average molecular weight of 270 was assumed for serum NEFAs. Non-oxidative glucose metabolism was calculated by subtracting the glucose oxidation rate (determined by indirect calorimetry) from R_d .

Percentage overweight was calculated as: $100 \times (\text{weight/ideal body weight}) - 100$. Ideal body weight for height was determined according to the Metropolitan Life Insurance tables (1983).

Statistical analysis

Data are presented as mean \pm SEM. Differences between day 2 and day 50% OWR, as well as differences between basal and insulin-stimulated biopsies were analysed by the Student's *t*-test for paired samples. Non-parametric (Wilcoxon signed-rank test) tests for paired samples were performed when appropriate. Correlation analysis was carried out using Pearson's correlation. All analyses were performed using SPSS for Windows version 12.0 (SPSS Inc., Chicago, IL, USA). Significance was accepted at $p < 0.05$.

RESULTS

Clinical and metabolic characteristics

Patient characteristics can be found in Table 1. Mean weight loss from day 2 to day 50% OWR amounted 20.3 ± 2.2 kg, average time to weight loss of 50% of overweight was 17 weeks (range 4 to 35 weeks). FPG levels declined significantly from day 2 to day 50% OWR (12.5 ± 0.5 to 7.8 ± 0.5 mmol/L, $p = 0.0001$). Basal EGP decreased from 20.0 ± 0.9 to 16.4 ± 1.2 $\mu\text{mol} \cdot \text{kgFFM}^{-1} \cdot \text{min}^{-1}$, $p = 0.001$. Weight loss to 50% OWR also improved insulin sensitivity (Table 2),

Table 1. Patient characteristics.

Sex (male/female)	2	:	8
Age (years)	54	\pm	3
Weight (kg)	113.0	\pm	7.1
BMI (kg/m ²)	40.2	\pm	1.6
Waist circumference (cm)	126.8	\pm	3.3
Fat mass (kg)	51.0	\pm	3.9
Fasting plasma glucose (mmol/L)	11.1	\pm	0.8
HbA _{1c} (%)	7.7	\pm	0.4
Duration type 2 diabetes (years)	8	\pm	3
Units of insulin injected per day	94	\pm	14
Additional use of oral glucose-lowering medication	8 metformin 2 rosiglitazone		

Data are presented as mean \pm SEM.

Table 2. Metabolic parameters during a VLCD on day 2 and after 50% reduction of overweight in obese type 2 diabetic patients.

	Day 2			Day 50% OWR		
	Basal	Clamp	P	Basal	Clamp	P
Glucose (mmol/L)	12.5 \pm 0.5	5.1 \pm 0.3	0.0001	7.8 \pm 0.5 [*]	5.4 \pm 0.3	0.003
Insulin (mU/L)	24.2 \pm 2.2	90.2 \pm 3.3	0.0001	15.2 \pm 1.3 [†]	80.8 \pm 4.0 [‡]	0.0001
NEFA (mmol/L)	1.6 \pm 0.2	1.1 \pm 0.3	NS	1.2 \pm 0.1 [§]	0.3 \pm 0.1	0.012
Triglycerides (mmol/L)	2.7 \pm 0.5	2.5 \pm 0.5	NS	1.2 \pm 0.1 [¶]	0.9 \pm 0.1 [¶]	0.0001
Glycerol ($\mu\text{mol/L}$)	150 \pm 15	114 \pm 18	NS	108 \pm 12 ^{**}	65 \pm 12 ^{††}	0.011
Glucose R _d ^Δ	20.0 \pm 0.9	18.8 \pm 2.0	NS	16.4 \pm 1.2 [†]	39.1 \pm 2.8 [†]	0.001
EGP ^Δ	20.0 \pm 0.9	8.5 \pm 0.9	0.0001	16.4 \pm 1.2 [†]	4.6 \pm 1.2 [¶]	0.0001
Glycerol R _a [□]	16.4 \pm 2.3	11.5 \pm 2.3	NS	14.6 \pm 1.4	7.5 \pm 1.6	0.012
Glucose oxidation ^{Δ□}	6.7 \pm 1.4	6.1 \pm 0.9	NS	4.2 \pm 0.4	12.7 \pm 1.5 ^{††}	0.001
NOGD ^Δ	14.8 \pm 1.1	12.2 \pm 1.6	NS	12.4 \pm 1.1 ^{§§}	27.7 \pm 2.8 ^{††}	0.005
Lipid oxidation ^Δ	8.0 \pm 0.5	8.3 \pm 0.3	NS	7.1 \pm 0.5	5.5 \pm 0.8 ^{**}	0.011

^Δ values in value in $\mu\text{mol} \cdot \text{kgFFM}^{-1} \cdot \text{min}^{-1}$; [□] value in $\mu\text{mol} \cdot \text{kgFFM}^{-1} \cdot \text{min}^{-1}$

NEFA = non-esterified fatty acids, R_d = rate of disappearance (= peripheral glucose disposal); EGP = endogenous glucose production,

NOGD = non-oxidative glucose disposal rate, FFM = fat free mass, FM = fat mass

Day 2 versus day 50% OWR:

^{*} $p = 0.0001$; [†] $p = 0.001$; [‡] $p = 0.023$; [§] $p = 0.018$; ^{||} $p = 0.017$; [¶] $p = 0.005$; ^{**} $p = 0.019$; ^{††} $p = 0.008$; ^{†††} $p = 0.011$; ^{††††} $p = 0.002$; ^{§§} $p = 0.036$

especially insulin-stimulated glucose disposal increased by 107% (18.8 ± 2.0 to 39.1 ± 2.8 $\mu\text{mol.kgFFM}^{-1}.\text{min}^{-1}$ ($p=0.001$)).

Effect of weight loss on insulin signalling in skeletal muscle

Absolute levels of insulin-stimulated IRS-1-associated PI3K were equal on both study days but the magnitude of the insulin-effect compared to basal was greater and only significantly enhanced after weight loss ($p = 0.01$, Fig. 1). To corroborate this finding, we also assessed the phosphorylation of two more distal components of the insulin signalling system, i.e., the recently identified PKB/Akt substrates AS160 and proline-rich Akt substrate 40 (PRAS40). Basal as well as insulin-stimulated AS160 phosphorylation, corrected for AS160 protein expression, was significantly higher after weight loss as compared to day 2 of the VLCD (Fig. 2). In addition, basal and hyperinsulinaemic levels of PRAS40 phosphorylation, were also significantly increased on day 50% OWR as compared to day 2 (Fig. 3).

Effect of weight loss on the fuel transporters GLUT-4 and FAT-36

Weight reduction had no significant effect on the abundance of the fuel transporters GLUT-4 (Fig. 4) and FAT/CD36 (Fig. 5) at the plasma membrane following hyperinsulinaemia. However, it should be noted that 7 out of the 10 patients showed a higher GLUT-4 density at the

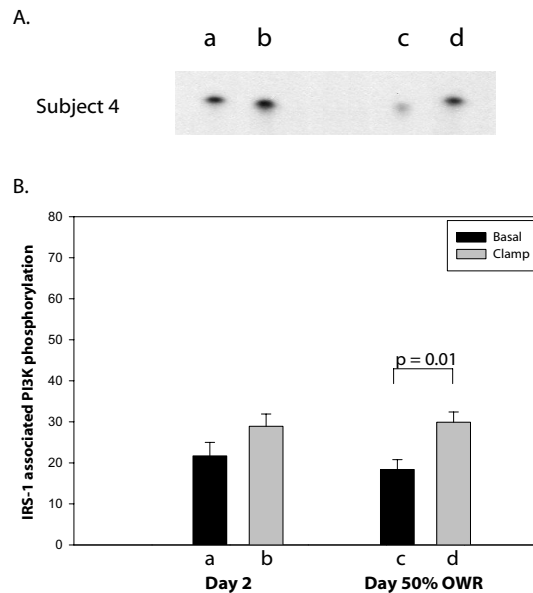


Figure 1

Immunoblot (A) and quantification (B) of IRS-1-associated PI3K activity in vastus lateralis muscle biopsies obtained on day 2 of a VLCD (a and b) and after 50% of overweight was lost (c and d) in basal (a and c) and hyperinsulinaemic euglycaemic conditions (b and d). Data are expressed as mean \pm SEM. Note that only insulin-stimulated increase over basal is significant on day 50% OWR.

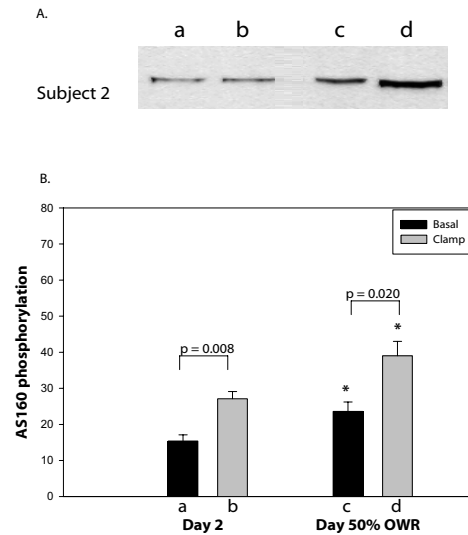


Figure 2

Immunoblot (A) and quantification (B) of AS160 phosphorylation in vastus lateralis muscle biopsies obtained on day 2 of a VLCD (a and b) and after 50% of overweight was lost with the VLCD (c and d) in basal (a and c) and hyperinsulinaemic (b and d) conditions. Data are expressed as mean \pm SEM.

Note the absolute increase in AS160 phosphorylation following weight loss, both in the basal as well as in the insulin-stimulated situation. *P = 0.026, day 50% OWR compared to day 2, basal as well as insulin-stimulated.

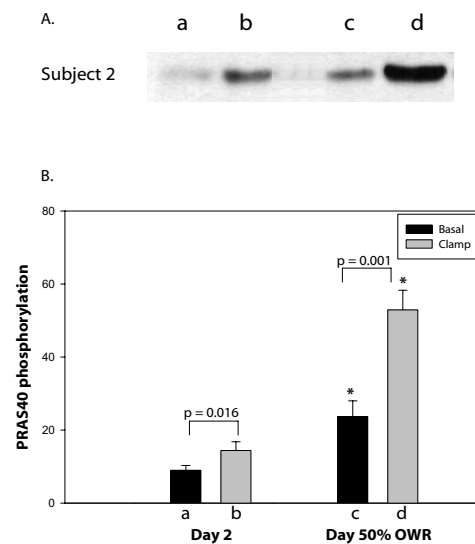


Figure 3

Immunoblot (A) and quantification (B) of PRAS40 phosphorylation in vastus lateralis muscle biopsies obtained on day 2 of a VLCD (a and b) and after 50% of overweight was lost with the VLCD (c and d) in basal (a and c) and hyperinsulinaemic (b and d) conditions. Data are expressed as mean \pm SEM.

Note that PRAS 40 phosphorylation is increased in the basal and insulin-stimulated situation after weight loss. *P = 0.046, †p = 0.018, day 50% OWR compared to day 2.

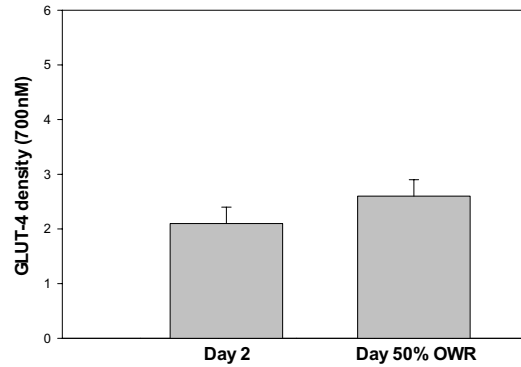


Figure 4

Quantification of GLUT-4 at the cell membrane during insulin-stimulated conditions on day 2 of a VLCD and after 50% of the overweight was lost with the VLCD (50% OWR). Data are expressed as mean \pm SEM. Changes between study days were not significant.

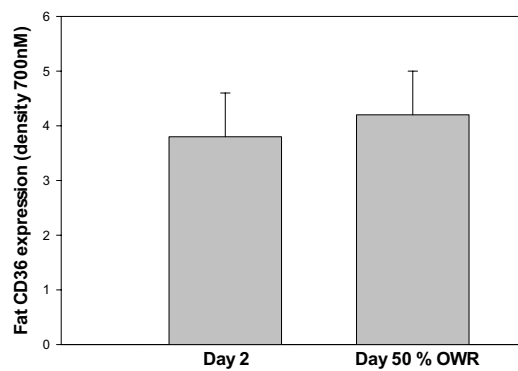


Figure 5

Quantification of FAT/CD36 at the cell membrane during insulin-stimulated conditions on day 2 of a VLCD and after 50% of the overweight was lost with the VLCD (50% OWR). Data are expressed as mean \pm SEM. Changes between study days were not significant.

cell membrane after weight loss. As to FAT/CD 36 the results were much less coherent: 4 patients showed an increase, 4 a decrease and 2 had equal FAT/CD36 expression at the cell membrane after weight loss.

In a correlation analysis, insulin-stimulated GLUT-4 content at the cell membrane did not correlate with the rate of glucose disposal on either study day. Neither did the change in insulin-stimulated sarcolemmal GLUT-4 content between study days correlate with the change in insulin-stimulated glucose disposal. Also no correlation between insulin-stimulated plasma-lemmal GLUT-4 content and body weight, age or duration of type 2 diabetes was found.

FAT/CD36 at the cell membrane during insulin infusion did not correlate with whole-body lipolysis, lipid oxidation or insulin-stimulated glucose disposal. However, a negative correlation was found between insulin stimulated sarcolemmal FAT/CD36 and the serum concentration of NEFAs during insulin stimulation ($r = -0.88$, $p = 0.004$ on day 2 and $r = -0.72$, $p = 0.045$).

Intramyocellular triglyceride content as assessed with an Oil red O Staining

Oil-red-O staining, as a measure of intramyocellular lipids, showed a reduction in intramyocellular lipids after weight loss (Fig. 6, Fig. 7). Type I and type II muscle fibres were also examined separately. Type I muscle fibres contained significantly more intramyocellular triglycerides on either study day as compared with type II muscle fibres. In both fibre types however, the amount of intramyocellular triglycerides decreased with weight loss. The percentage type I fibres did not change with weight loss although a slight, non-significant increase was observed ($46.8 \pm 4.9\%$ to $51.5 \pm 4.1\%$, $p = \text{NS}$, Fig. 7B), and accordingly, a decrease in type II muscle fibres. Interestingly, time to weight loss of 50% overweight correlated negatively with the number of type I fibres at the start of the diet (day 2), $r = -0.64$, $p = 0.046$. The amount of intramyocellular triglycerides correlated significantly with lipid oxidation ($r = 0.74$, $p = 0.024$) and whole-body insulin-stimulated glucose disposal (negative correlation, $r = -0.63$, $p = 0.049$) on day 50% OWR. In addition, the change in intramyocellular triglyceride concentration did not correlate with change in body weight, glucose and lipid metabolism (variables as shown in Table 2), insulin signalling or FAT/CD36 content.

DISCUSSION

This study shows that, as opposed to a 2-day VLCD, which only decreased basal EGP, prolonged caloric restriction leading to a loss of 50% of overweight also improves insulin sensitivity, especially insulin-stimulated glucose disposal (see Chapter 8 for the discussion of the clamp studies). Over 80% of insulin-stimulated glucose disposal takes place in skeletal muscle¹, with glucose transport over the membrane being the rate-limiting step². We found improved insulin signalling, reflected by a small insulin-stimulated increase over basal with respect to IRS-1-associated PI3K activity and a clear absolute increase in two of its downstream components, AS160 and PRAS40. The amount of GLUT-4 at the cell membrane during insulin stimulation showed a tendency to increase after weight loss, however, this small increase in sarcolemmal GLUT-4 seems not in accordance with the clear improvement (107% increase as compared to day 2) in insulin-stimulated glucose disposal.

The reason why the increase in insulin-stimulated glucose disposal at the whole-body level was not reflected by a significant improvement in GLUT-4 translocation to the cell membrane is unclear and may reflect changes in intrinsic activity of GLUT-4. Others have also reported a dissociation between insulin-stimulated glucose disposal and either insulin signalling and/or GLUT-4 content at the cell membrane. Ryder *et al.*⁷ found that although insulin-stimulated glucose disposal was 50% lower in patients with type 2 diabetes compared with lean controls, insulin-stimulated cell surface GLUT-4 content over basal amounted only 10% that of healthy controls in type 2 diabetic patients. In another study, Karlsson *et al.* found a significant, 36% improvement in insulin-stimulated whole-body glucose uptake after 26 weeks of

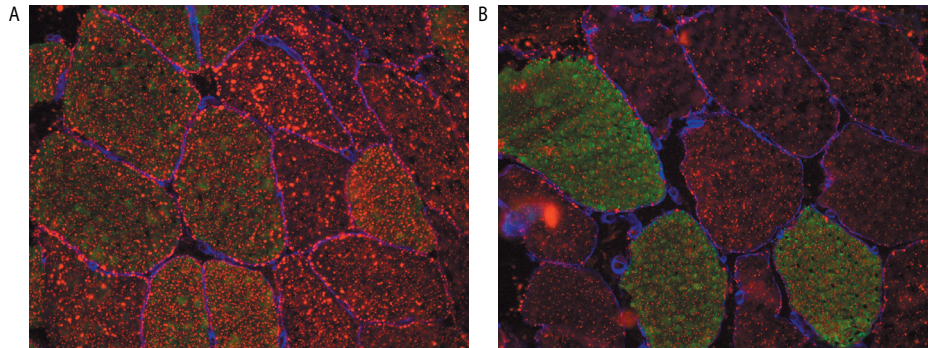


Figure 6
Oil red O staining (red) in combination with myosin heavy chain type 1 (MHC-1) immunofluorescence (green) and lamin staining (blue) in cryosections of vastus lateralis muscle on day 2 of a VLCD (A) and after 50% of overweight was lost with the VLCD (B). Note the decrease in intramyocellular triglyceride content on day 50% OWR (Fig. 6B).

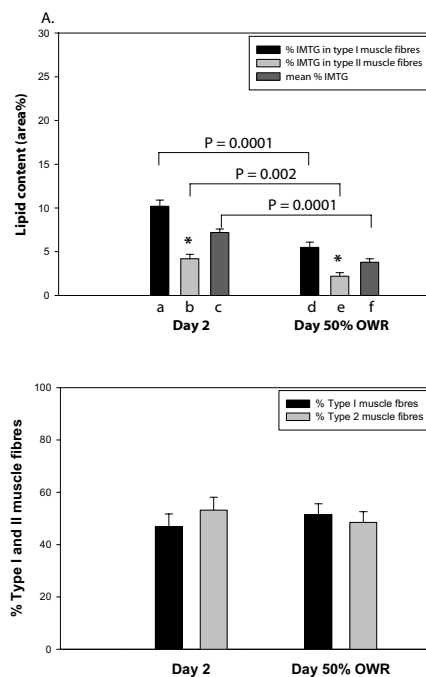


Figure 7
Quantification of the percentage intramyocellular triglycerides (IMTG, Fig. 7A) in type I muscle fibres (black bars), type II muscle fibres (light grey bars) and mean % IMTG (i.e., type I and II fibres combined, dark grey bars) on day 2 (a,b,c) of a VLCD and after 50% of overweight was lost (d,e,f). Note the significant decrease in IMTG after weight loss in both fibre types. Figure 7B shows the number of type I (black bars) and type II (grey bars) fibres on either study day. Note the significant increase in type I muscle fibres after weight loss.

treatment with 8 mg rosiglitazone daily in newly diagnosed type 2 diabetic patients, that was not accompanied by improved signalling of IRS-1 associated PI3K, PKB/AKT or AS160³⁴. Finally, Friedman *et al.*³⁵ showed that weight loss of 36% of initial body weight by gastric

bypass surgery improved whole-body glucose disposal by 3-fold and maximal glucose transport activity *in vitro* by 50% in 3 non-diabetic and 4 type 2 diabetic morbidly obese individuals, without an effect on total GLUT-4 protein content in skeletal muscle biopsies. Collectively, this indicates that not the amount of GLUT-4 at the cell membrane but its function and, consequently, the velocity of glucose transport over the membrane are the main determinants of insulin-stimulated glucose disposal. Alternatively, another glucose transporter, either GLUT-1⁷, or a yet unidentified one, may have contributed to the increase in glucose uptake seen after weight loss. Another possible explanation is that insulin-stimulated glucose disposal in adipose tissue is greatly enhanced with weight loss. In 4 out of 8 patients from whom we obtained abdominal subcutaneous adipose tissue biopsies, an increase in insulin-stimulated PI3K-activity was observed after weight loss (data not shown).

Insulin-stimulated phosphorylation of AS160, a recently discovered substrate of PKB/Akt, has previously been reported to be disturbed in skeletal muscle of moderately obese (BMI 27 kg/m²) type 2 diabetic patients with relatively mild diabetes (9 out of 10 used oral agents, only 1 patient on insulin therapy, HbA_{1c} 6.0 ± 0.5%)¹⁷. We did not use control subjects and can therefore not compare insulin-stimulated AS160 phosphorylation in our patients with that of healthy lean subjects. However, our patients were much more obese (BMI 40.2 ± 1.6 kg/m²) and severely insulin-resistant (glucose disposal rate 18.8 ± 2.0 μmol.kgFFM⁻¹.min⁻¹; M-value 9.9 ± 2.3 μmol.kgFFM⁻¹.min⁻¹) as the patients in the study mentioned above¹⁷ and, notwithstanding, we found a significant effect of insulin on AS160 phosphorylation on both study days. This study also shows that significant weight reduction (50% of overweight) enhances insulin-stimulated AS160 phosphorylation.

Notably, we observed that weight reduction significantly increases insulin-stimulated PRAS 40 phosphorylation, another substrate for PKB/Akt. PRAS40 is a nuclear protein,^{36,37} and phosphorylation of PRAS40 facilitates the binding of 14-3-3-proteins *in vitro*. Studies in animal models and cultured cell lines suggest that PRAS40 regulates cell survival and protection from ischaemia. Although the physiological function of PRAS40 in insulin action is still unclear, we recently observed that phosphorylation of this protein is induced by physiological hyperinsulinaemia in insulin target tissues, and blunted under conditions of high-fat-diet-induced insulin resistance (E.B.M. Nascimento *et al.*, submitted). Together, these findings suggest an important role for PRAS40 in physiological insulin action.

It has been hypothesised, that accumulation of intramyocellular lipids (IMCLs) are involved in the cause of impaired insulin signalling via phosphorylation of IRS-1 and IRS-2 on serine residues by fatty acid metabolites, thereby rendering these serine-phosphorylated IRSs unable to associate with and activate PI3K⁴¹. In our study substantial weight loss was associated with a significant decrease in IMCL. Only intramyocellular lipid content on day 50% OWR correlated negatively with the glucose disposal rate, but not with any other metabolic parameter we measured, nor with insulin signalling. Indeed, several other studies have also reported a decrease in IMCL following substantial weight reduction after bariatric surgery in

morbidly obese, non-diabetic subjects³⁹⁻⁴¹, which was also associated with improved insulin-stimulated glucose disposal. On the other hand, more moderate weight loss (approximately 8 to 10 kg) in obese patients did not affect total IMCL content in 2 other studies^{42,43}. In obese type 2 diabetic patients, Goodpaster *et al.* found a 41% reduction in IMCL following weight loss of approximately 14 kg⁴⁴.

Several studies have shown that patients with type 2 diabetes have a decreased percentage type I (oxidative) muscle fibres and an increased percentage type IIb (glycolytic) muscle fibres^{45,46}, like in our patients. A low capacity to oxidise fat due to a low percentage of type I muscle fibres might lead to obesity. However, whether the altered fibre type composition is the cause of obesity and type 2 diabetes or an effect of these pathologic states is unclear. Weight loss resulted in a slight, albeit non-significant, increase in the percentage of type I (and hence decrease in type II) muscle fibres. Only one other study⁴⁷ reported a tendency to increased type I fibres following weight loss, whereas the remainder of studies showed no changes in type I muscle fibres with weight loss⁴⁸⁻⁵⁰. None of these studies were performed in type 2 diabetic patients however. Interestingly, like one other study⁵¹, we also found a positive relation between the amount of type I (oxidative) muscle fibres on day 2 and time to loss of 50% of overweight. The fact that type I muscle fibres contain more IMCL than type II muscle fibres and that IMCL in both muscle type fibres decrease with weight loss has been observed before⁴⁷.

IMCL might accumulate *via* increased fatty acid uptake and/or decreased fatty acid oxidation and/or –re-esterification. Weight loss did not change the amount of the fatty acid transporter FAT/CD36 at the cell membrane in our study (if any it was a tendency to increase). This is in contradiction with the hypothesis of Bonen *et al.*, who observed an increased sarcolemmal expression of FAT/CD36 in skeletal muscle of obese and type 2 diabetic patients along with an increased long-chain fatty acid uptake and proposed that this could contribute to increased IMCL and hence impaired insulin signalling⁵². With this hypothesis in mind, beforehand we expected to find a decreased sarcolemmal expression of FAT/CD36 after substantial weight loss. However, like GLUT-4, FAT/CD36 traffics between the sarcolemma and the cytoplasm and has even been demonstrated in mitochondria⁵³. The trafficking can be regulated by insulin and exercise, involving PI3K/Akt⁵⁴ and adenosine monophosphate activated protein kinase (AMPK)⁵⁴ signalling pathways, respectively. Therefore, a weight-loss-induced improvement in insulin signalling could also enhance insulin-induced FAT/CD36 translocation to the sarcolemma. However, in our study, insulin-stimulated sarcolemmal FAT/CD36 did not change. Plasma NEFA levels and IMCL decreased, in combination with a decrease in whole-body lipolysis and lipid oxidation. Although highly speculative, one could assume that as a consequence of the considerable loss of adipose tissue whereby a new steady state has developed in our patients, the total release of NEFAs by fat cells is diminished and, therefore, the uptake by myocytes, leading to decreased IMCL and lipid oxidation.

In conclusion, substantial weight loss in obese, insulin-treated type 2 diabetic patients, improves insulin sensitivity of skeletal muscle, adipose tissue and the liver. Especially insulin-stimulated glucose disposal improved considerably. At the cellular level, this was accompanied by improved insulin signalling. The observed decrease in IMCL might have contributed to the improved insulin signalling.

REFERENCES

1. DeFronzo RA, Jacot E, Jequier E, Maeder E, Wahren J, Felber JP. The effect of insulin on the disposal of intravenous glucose. Results from indirect calorimetry and hepatic and femoral venous catheterization. *Diabetes* 1981; 30(12):1000-1007.
2. Ziel FH, Venkatesan N, Davidson MB. Glucose transport is rate limiting for skeletal muscle glucose metabolism in normal and STZ-induced diabetic rats. *Diabetes* 1988; 37(7):885-890.
3. Bjornholm M, Kawano Y, Lehtihet M, Zierath JR. Insulin receptor substrate-1 phosphorylation and phosphatidylinositol 3-kinase activity in skeletal muscle from NIDDM subjects after in vivo insulin stimulation. *Diabetes* 1997; 46(3):524-527.
4. Kim YB, Nikoulina SE, Ciaraldi TP, Henry RR, Kahn BB. Normal insulin-dependent activation of Akt/protein kinase B, with diminished activation of phosphoinositide 3-kinase, in muscle in type 2 diabetes. *J Clin Invest* 1999; 104(6):733-741.
5. Cusi K, Maezono K, Osman A, Pendergrass M, Patti ME, Pratipanawatr T et al. Insulin resistance differentially affects the PI 3-kinase- and MAP kinase-mediated signaling in human muscle. *J Clin Invest* 2000; 105(3):311-320.
6. Krook A, Bjornholm M, Galuska D, Jiang XJ, Fahlman R, Myers MG, Jr. et al. Characterization of signal transduction and glucose transport in skeletal muscle from type 2 diabetic patients. *Diabetes* 2000; 49(2):284-292.
7. Ryder JW, Yang J, Galuska D, Rincon J, Bjornholm M, Krook A et al. Use of a novel impermeable biotinylated photolabeling reagent to assess insulin- and hypoxia-stimulated cell surface GLUT4 content in skeletal muscle from type 2 diabetic patients. *Diabetes* 2000; 49(4):647-654.
8. Koistinen HA, Galuska D, Chibalin AV, Yang J, Zierath JR, Holman GD et al. 5-amino-imidazole carboxamide riboside increases glucose transport and cell-surface GLUT4 content in skeletal muscle from subjects with type 2 diabetes. *Diabetes* 2003; 52(5):1066-1072.
9. Handberg A, Vaag A, Damsbo P, Beck-Nielsen H, Vinten J. Expression of insulin regulatable glucose transporters in skeletal muscle from type 2 (non-insulin-dependent) diabetic patients. *Diabetologia* 1990; 33(10):625-627.
10. Pedersen O, Bak JF, Andersen PH, Lund S, Moller DE, Flier JS et al. Evidence against altered expression of GLUT1 or GLUT4 in skeletal muscle of patients with obesity or NIDDM. *Diabetes* 1990; 39(7):865-870.
11. Beeson M, Sajan MP, Dizon M, Grebenev D, Gomez-Daspert J, Miura A et al. Activation of protein kinase C-zeta by insulin and phosphatidylinositol-3,4,5-(PO4)3 is defective in muscle in type 2 diabetes and impaired glucose tolerance: amelioration by rosiglitazone and exercise. *Diabetes* 2003; 52(8):1926-1934.
12. Krook A, Roth RA, Jiang XJ, Zierath JR, Wallberg-Henriksson H. Insulin-stimulated Akt kinase activity is reduced in skeletal muscle from NIDDM subjects. *Diabetes* 1998; 47(8):1281-1286.
13. Brozinick JT, Jr., Roberts BR, Dohm GL. Defective signaling through Akt-2 and -3 but not Akt-1 in insulin-resistant human skeletal muscle: potential role in insulin resistance. *Diabetes* 2003; 52(4):935-941.
14. Kane S, Sano H, Liu SC, Asara JM, Lane WS, Garner CC et al. A method to identify serine kinase substrates. Akt phosphorylates a novel adipocyte protein with a Rab GTPase-activating protein (GAP) domain. *J Biol Chem* 2002; 277(25):22115-22118.

15. Sano H, Kane S, Sano E, Miinea CP, Asara JM, Lane WS et al. Insulin-stimulated phosphorylation of a Rab GTPase-activating protein regulates GLUT4 translocation. *J Biol Chem* 2003; 278(17):14599-14602.
16. Zeigerer A, McBrayer MK, McGraw TE. Insulin stimulation of GLUT4 exocytosis, but not its inhibition of endocytosis, is dependent on RabGAP AS160. *Mol Biol Cell* 2004; 15(10):4406-4415.
17. Karlsson HK, Zierath JR, Kane S, Krook A, Lienhard GE, Wallberg-Henriksson H. Insulin-stimulated phosphorylation of the Akt substrate AS160 is impaired in skeletal muscle of type 2 diabetic subjects. *Diabetes* 2005; 54(6):1692-1697.
18. Jazet IM, Pijl H, Frolich M, Romijn JA, Meinders AE. Two days of a very low calorie diet reduces endogenous glucose production in obese type 2 diabetic patients despite the withdrawal of blood glucose-lowering therapies including insulin. *Metabolism* 2005; 54(6):705-712.
19. Jazet IM, Ouwens DM, Schaart G, Pijl H, Keizer HA, Maassen JA et al. Effect of a 2-day very low-energy diet on skeletal muscle insulin sensitivity in obese type 2 diabetic patients on insulin therapy. *Metabolism* 2005.
20. Andersson BL, Bjorntorp P, Seidell JC. Measuring Obesity-Classification and description of anthropometric data. Report on a WHO consultation on epidemiology of obesity. Copenhagen. Nutrition unit, WHO regional office for Europe; EUR/ICP/NUT. 125, 1-22. 1988.
21. Hother-Nielsen O, Beck-Nielsen H. On the determination of basal glucose production rate in patients with type 2 (non-insulin-dependent) diabetes mellitus using primed- continuous 3-3H-glucose infusion. *Diabetologia* 1990; 33(10):603-610.
22. DeFronzo RA, Tobin JD, Andres R. Glucose clamp technique: a method for quantifying insulin secretion and resistance. *Am J Physiol* 1979; 237(3):E214-E223.
23. Reinauer H, Gries FA, Hubinger A, Knode O, Severing K, Susanto F. Determination of glucose turnover and glucose oxidation rates in man with stable isotope tracers. *J Clin Chem Clin Biochem* 1990; 28(8):505-511.
24. Ackermans MT, Ruiter AF, Endert E. Determination of glycerol concentrations and glycerol isotopic enrichments in human plasma by gas chromatography/mass spectrometry. *Anal Biochem* 1998; 258(1):80-86.
25. Bergstrom J. Percutaneous needle biopsy of skeletal muscle in physiological and clinical research. *Scand J Clin Lab Invest* 1975; 35(7):609-616.
26. Hickey MS, Tanner CJ, O'Neill DS, Morgan LJ, Dohm GL, Houmard JA. Insulin activation of phosphatidylinositol 3-kinase in human skeletal muscle in vivo. *J Appl Physiol* 1997; 83(3):718-722.
27. Ouwens DM, Zon GC van der, Pronk GJ, Bos JL, Moller W, Cheatham B et al. A mutant insulin receptor induces formation of a Shc-growth factor receptor bound protein 2 (Grb2) complex and p21ras-GTP without detectable interaction of insulin receptor substrate 1 (IRS1) with Grb2. Evidence for IRS1-independent p21ras-GTP formation. *J Biol Chem* 1994; 269(52):33116-33122.
28. Koopman R, Schaart G, Hesselink MK. Optimisation of oil red O staining permits combination with immunofluorescence and automated quantification of lipids. *Histochem Cell Biol* 2001; 116(1):63-68.
29. Roorda BD, Hesselink MK, Schaart G, Moonen-Kornips E, Martinez-Martinez P, Losen M et al. DGAT1 overexpression in muscle by in vivo DNA electroporation increases intramyocellular lipid content. *J Lipid Res* 2005; 46(2):230-236.

30. Borghouts LB, Schaart G, Hesselink MK, Keizer HA. GLUT-4 expression is not consistently higher in type-1 than in type-2 fibres of rat and human vastus lateralis muscles; an immunohistochemical study. *Pflugers Arch* 2000; 441(2-3):351-358.
31. Keizer HA, Schaart G, Tandon NN, Glatz JF, Luiken JJ. Subcellular immunolocalisation of fatty acid translocase (FAT)/CD36 in human type-1 and type-2 skeletal muscle fibres. *Histochem Cell Biol* 2004; 121(2):101-107.
32. Steele R. Influences of glucose loading and of injected insulin on hepatic glucose output. *Ann N Y Acad Sci* 1959; 82:420-430.
33. Simonson DC, DeFronzo RA. Indirect calorimetry: methodological and interpretative problems. *Am J Physiol* 1990; 258(3 Pt 1):E399-E412.
34. Karlsson HK, Hallsten K, Bjornholm M, Tsuchida H, Chibalin AV, Virtanen KA et al. Effects of metformin and rosiglitazone treatment on insulin signaling and glucose uptake in patients with newly diagnosed type 2 diabetes: a randomized controlled study. *Diabetes* 2005; 54(5):1459-1467.
35. Friedman JE, Dohm GL, Leggett-Frazier N, Elton CW, Tapscott EB, Pories WP et al. Restoration of insulin responsiveness in skeletal muscle of morbidly obese patients after weight loss. Effect on muscle glucose transport and glucose transporter GLUT4. *J Clin Invest* 1992; 89(2):701-705.
36. Kovacina KS, Park GY, Bae SS, Guzzetta AW, Schaefer E, Birnbaum MJ et al. Identification of a proline-rich Akt substrate as a 14-3-3 binding partner. *J Biol Chem* 2003; 278(12):10189-10194.
37. Beausoleil SA, Jedrychowski M, Schwartz D, Elias JE, Villen J, Li J et al. Large-scale characterization of HeLa cell nuclear phosphoproteins. *Proc Natl Acad Sci U S A* 2004; 101(33):12130-12135.
38. Perseghin G, Petersen K, Shulman GI. Cellular mechanism of insulin resistance: potential links with inflammation. *Int J Obes Relat Metab Disord* 2003; 27 Suppl 3:S6-11.
39. Fabris R, Mingrone G, Milan G, Manco M, Granzotto M, Dalla PA et al. Further lowering of muscle lipid oxidative capacity in obese subjects after biliopancreatic diversion. *J Clin Endocrinol Metab* 2004; 89(4):1753-1759.
40. Greco AV, Mingrone G, Giancaterini A, Manco M, Morroni M, Cinti S et al. Insulin resistance in morbid obesity: reversal with intramyocellular fat depletion. *Diabetes* 2002; 51(1):144-151.
41. Houmard JA, Tanner CJ, Yu C, Cunningham PG, Pories WJ, MacDonald KG et al. Effect of weight loss on insulin sensitivity and intramuscular long-chain fatty acyl-CoAs in morbidly obese subjects. *Diabetes* 2002; 51(10):2959-2963.
42. Petersen KF, Dufour S, Befroy D, Lehrke M, Hendler RE, Shulman GI. Reversal of nonalcoholic hepatic steatosis, hepatic insulin resistance, and hyperglycemia by moderate weight reduction in patients with type 2 diabetes. *Diabetes* 2005; 54(3):603-608.
43. He J, Goodpaster BH, Kelley DE. Effects of weight loss and physical activity on muscle lipid content and droplet size. *Obes Res* 2004; 12(5):761-769.
44. Goodpaster BH, Theriault R, Watkins SC, Kelley DE. Intramuscular lipid content is increased in obesity and decreased by weight loss. *Metabolism* 2000; 49(4):467-472.
45. Hickey MS, Carey JO, Azevedo JL, Houmard JA, Pories WJ, Israel RG et al. Skeletal muscle fiber composition is related to adiposity and in vitro glucose transport rate in humans. *Am J Physiol* 1995; 268(3 Pt 1):E453-E457.
46. Marin P, Andersson B, Krotkiewski M, Bjorntorp P. Muscle fiber composition and capillary density in women and men with NIDDM. *Diabetes Care* 1994; 17(5):382-386.

47. Niskanen L, Uusitupa M, Sarlund H, Siitonen O, Paljarvi L, Laakso M. The effects of weight loss on insulin sensitivity, skeletal muscle composition and capillary density in obese non-diabetic subjects. *Int J Obes Relat Metab Disord* 1996; 20(2):154-160.
48. Gray RE, Tanner CJ, Pories WJ, MacDonald KG, Houmard JA. Effect of weight loss on muscle lipid content in morbidly obese subjects. *Am J Physiol Endocrinol Metab* 2003; 284(4):E726-E732.
49. Kern PA, Simsolo RB, Fournier M. Effect of weight loss on muscle fiber type, fiber size, capillarity, and succinate dehydrogenase activity in humans. *J Clin Endocrinol Metab* 1999; 84(11):4185-4190.
50. Kempen KP, Saris WH, Kuipers H, Glatz JF, Vusse GJ van der. Skeletal muscle metabolic characteristics before and after energy restriction in human obesity: fibre type, enzymatic beta-oxidative capacity and fatty acid-binding protein content. *Eur J Clin Invest* 1998; 28(12):1030-1037.
51. Tanner CJ, Barakat HA, Dohm GL, Pories WJ, MacDonald KG, Cunningham PR et al. Muscle fiber type is associated with obesity and weight loss. *Am J Physiol Endocrinol Metab* 2002; 282(6):E1191-E1196.
52. Bonen A, Parolin ML, Steinberg GR, Calles-Escandon J, Tandon NN, Glatz JF et al. Triacylglycerol accumulation in human obesity and type 2 diabetes is associated with increased rates of skeletal muscle fatty acid transport and increased sarcolemmal FAT/CD36. *FASEB J* 2004; 18(10):1144-1146.
53. Bezaire V, Bruce CR, Heigenhauser GJ, Tandon NN, Glatz JF, Luiken JJ et al. Identification of fatty acid translocase on human skeletal muscle mitochondrial membranes: essential role in fatty acid oxidation. *Am J Physiol Endocrinol Metab* 2005.
54. Luiken JJ, Coort SL, Koonen DP, Bonen A, Glatz JF. Signalling components involved in contraction-inducible substrate uptake into cardiac myocytes. *Proc Nutr Soc* 2004; 63(2):251-258.